Morphometric, Gravity and Bathymetric (Topographic) Analysis of Bayana Basin, Rajasthan, India

Kutubuddin Ansari, Mery Biswas, Suvashree Das, and Soumyajit Mukherjee

Abstract The Bayana basin has been analyzed morphometrically considering five watersheds. Watershed 4 is found out to be highly active tectonically. We also analyzed gravity and bathymetric (topographic) variation in the basin. The result shows positive anomalies at places (~50 mGal) indicating either uplifted basement blocks or the presence of denser igneous bodies. Negative anomalies are noticed up to -35 mGal over areas with thicker sedimentary sequences or less dense materials. The bathymetry (topographic) elevation is lowest around 200 m near the Bayana town compared to the surrounding region which reaches up to ~ 1000 m. This kind of elevated distribution indicates a relatively steep gradient along the basin's eastern side, while the western side shows a more gradual slope. We investigate the *empirical orthogonal function* (EOF)-based gravity modeling and an analytical solution of gravity. The gravity as a function of bathymetry (topography) is estimated and the results are examined.

Keywords Morphometry · Basin tectonics · Empirical orthogonal function · Gravity · Bathymetry

1 Introduction

Rajasthan basins have received tremendous attention in India for hydrocarbon exploration and for academic research (e.g., Dasgupta and Mukherjee 2017; Kar et al., 2022, 2025; Dasgupta 2023; Dasgupta et al., 2023, 2024; Mishra et al., 2023; Puniya

K. Ansari
Integrated Geoinformation (IntGeo) Solution Private Limited, New Delhi, India

M. Biswas · S. Das
Department of Geography, Presidency University, Kolkata, India

S. Mukherjee (✉)
Department of Earth Sciences, Indian Institute of Technology Bombay, Powai, Mumbai, Maharashtra, India
e-mail: smukherjee@iitb.ac.in; soumyajitm@gmail.com

S. Mukherjee and N. R. Kar (eds.), *Geosciences of the Rajasthan Basins, India*, Springer Geology, https://doi.org/10.1007/978-981-96-3005-9_3

et al., 2023a,b; Ansari et al., 2024, 2025a, b, c; Biswas et al., 2022a, b, 2024; Raha et al., 2025). The Bayana basin is composed of a mostly undeformed and low-metamorphosed Proterozoic siliciclastic sediments belonging to the Delhi Supergroup (Miall 2006; Ahmad et al., 2012; Kumar and Kumar 2012; Raza et al., 2012). This section is dissected by rivers with different drainage patters at places having structural controls.

Through morphometric studies involving river courses in a terrain, one can comment on different degree of tectonic activeness within different watersheds of the terrain (review in Shekar and Mathew 2024). On the other hand, analysis of Earth's gravity field is important, used to implement for vertical reference frame and provides insights into mass distribution in the Earth system (Zingerle et al., 2020). High-resolution and precise gravity models are essential for global height unification and sea-level consistency (Gruber et al., 2012; Ihde et al. 2017). The gravity field can be applied as a surface of the physical reference frame in oceanographic applications to derive the mean of dynamic topography (Siegismund, 2013). The information obtained from gravity is also used for lithospheric modeling where it assists boundary value (McKenzie et al. 2014). The main contribution of change is gravity, which is induced by geodynamical events because of earthquakes and volcanoes, that can directly affect the gravity field. Since these events occur temporally, their cumulative changes affect significantly (Greco et al., 2021).

In the current study, we considered the gravity model based on empirical orthogonal function (EOF). An EOF is a statistical method that decomposes data into orthogonal basis functions. It is also known as principal component analysis and proper orthogonal decomposition. The EOF analysis is designed to find the coverability within a dataset and create new composite variables that capture that internal dependence, allowing a few composite uncorrelated variables to describe most of the variability in the data described in the much larger dependent data set (Martinson, 2018). The free-air gravity (FAG) anomaly data has been accessed from EGM2008 (Internet Ref-1, 2023) and used as covariable data (in the order latitude × longitude) set. The bathymetry elevation height data has been collected from the General Bathymetric Chart of the Oceans (GEBCO) (Internet Ref-2, 2023) in the regional area (latitude × longitude) and used to create the new composite variable.

2 Aim, Approach and Theory

2.1 Morphometry

Through morphometric studies, one can efficiently explain active tectonics (e.g., Raha et al., 2023). We performed morphotectonic analysis (based on Internet ref-3, 2024) of the Bayana basin considering six watershed-scale indicators. These are (*i*) transverse topographic symmetry (T), (*ii*) drainage basin asymmetry (AF), (*iii*) basin shape index (Bs), (*iv*) circularity ratio (*Rc*), (*v*) hypsometric integral (*HI*) and (*vi*) tilt angle (Θ) (Dasgupta et al., 2022; Biswas et al., 2022a, b; Raha et al., 2023; Mondal et al., 2024). We used the Copernicus Global Digital Elevation Model (Internet ref-3, 2024).

2.2 Geophysical Studies

Consider gravity observation matrix (g) for an area is arranged in the order latitude × longitude form. It is not necessary that the given matrix g will be a square matrix, hence consider another gravity observation G as follows (Jamjareegulgarn et al., 2020):

$$G = g \times g' \tag{1}$$

The base functions U_g or the eigenvectors of the matrix of g can be obtained by decomposing G (Ansari et al., 2024, 2025a, b, c):

$$G \times U_g = \lambda_g \times U_g \tag{2}$$

Here the associated eigenvalues are presented by λ_g. Once the EOF base function is understood, the EOF coefficients A_g can be obtained using following equation (Jamjareegulgarn et al., 2020; Ansari et al., 2024, 2025a, b, c):

$$A_g = g' \times U_g \tag{3}$$

Similarly, in case of Bathymetry dataset, consider the elevation height matrix (g) area to be arranged in the order latitude × longitude form and there is a matrix H is given by (Jamjareegulgarn et al., 2020):

$$H = h \times h' \tag{4}$$

The base functions U_h or the eigenvectors of the matrix of h with the associated eigenvalues (λ_h) can be obtained by decomposing H.

$$H \times U_h = \lambda_h \times U_h \tag{5}$$

and the form of EOF base function A_h can be abstained by using following equation (Ansari et al., 2024, 2025a, b, c):

$$A_h = h' \times U_h \tag{6}$$

The complete analytical expression of gravity effect on uncompensated bathymetry topographic height is given by (Parker, 1973):

$$g_{\text{Bathymetry}}(k) = 2\pi G(\rho_m - \rho_c)e^{-\text{kd}} \sum_{n=1}^{\infty} \frac{k^{n-1}}{n!} F(h^n) \tag{7}$$

Here ρ_m and ρ_c are the densities of the mantle and the crust in gm cm^{-3}. The Newton gravitational constant is indicated by G (m^3 kg^{-1} s^{-2}) and an undulating bathymetry Fourier transform by $F(h)$, d is the mean mantle depth (in km) and k the wave number in km^{-1}. Here n stands for the order of the equation. Putting $n = 1$ in Eq. (7), we get the first-order expression of the analytical solution (Watts, 2001).

$$g_{\text{Bathymetry}}(k) = 2\pi G(\rho_m - \rho_c)e^{-\text{kd}} F(h) \tag{8}$$

Relacing gravity$_{\text{Bathymetry}}$ with Bathymetry gravity base function (A_{gb}) and $F(h)$ by elevation height estimated base function in Eq. (8). Now the new obtained equation will be:

$$A_{\text{gb}} = 2\pi G(\rho_m - \rho_c)e^{-\text{kd}} A_h \tag{9}$$

Now the new gravity measurement matrix, which will be a function of Bathymetry elevation height (g_b) will be obtained (Jamjareegulgarn et al., 2020; Ansari et al., 2024, 2025a, b, c):

$$g_b = A_{\text{gb}} \times U_{g'} \tag{10}$$

The obtained gravity results (g_b) will be the function of Bathymetry elevation height.

3 Results

3.1 Geomorphological Aspects

These parameters are calculated with respect to five delineated watersheds (Fig. 1) in the Bayana basin. The slope aspect map (Fig. 2) discloses the directions of slope in the basin. Four drainage patterns (trellis, rectangular, radial with angular joining of streams and dendritic) are found (Fig. 3). Figure 4 shows the *index of active tectonics* (IAT), where watershed 4 is under class1 (IAT < 2) (tectonically highly active). Watersheds 2, 3 and 5 have IAT = 2–2.1. These watersheds come under class 2 (moderate tectonic activity). Watershed 4 belongs to class 3 with IAT > 2.1 (low tectonic activity) (Fig. 4). The Kernel spatial lineament density map and line density map also disclose that the rivers mostly follow the lineaments in the middle and in the western sections of the basin (Fig. 5a,b).

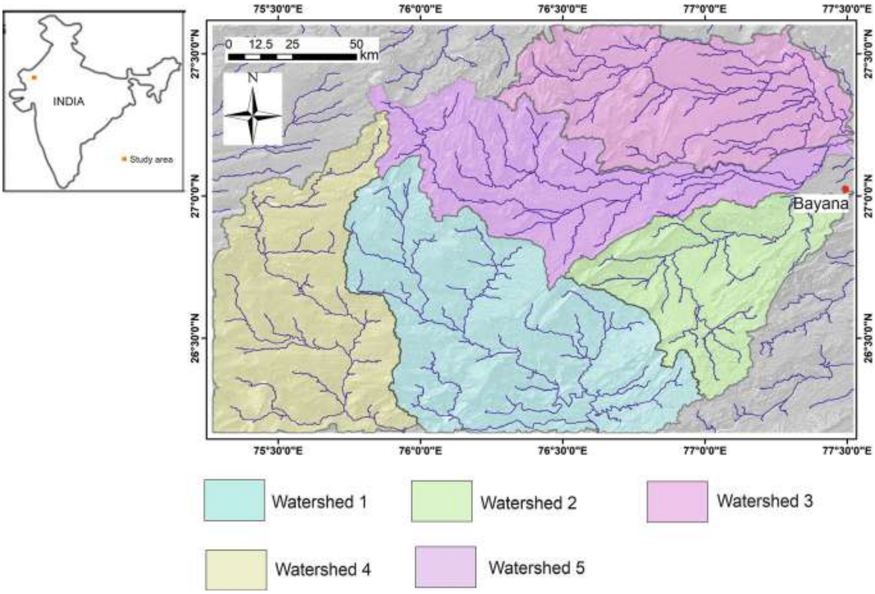

Fig. 1 Location of the Bayana basin with the five delineated watersheds

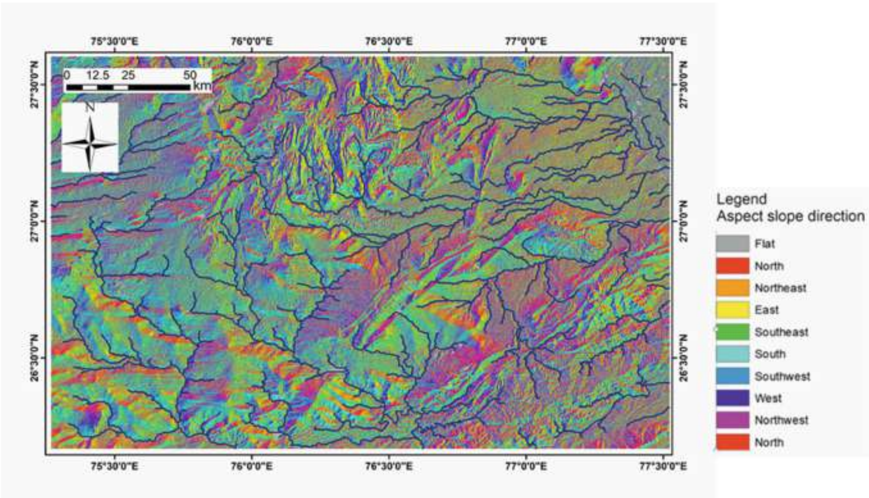

Fig. 2 Aspect slope map with drainage network showing the slope directions

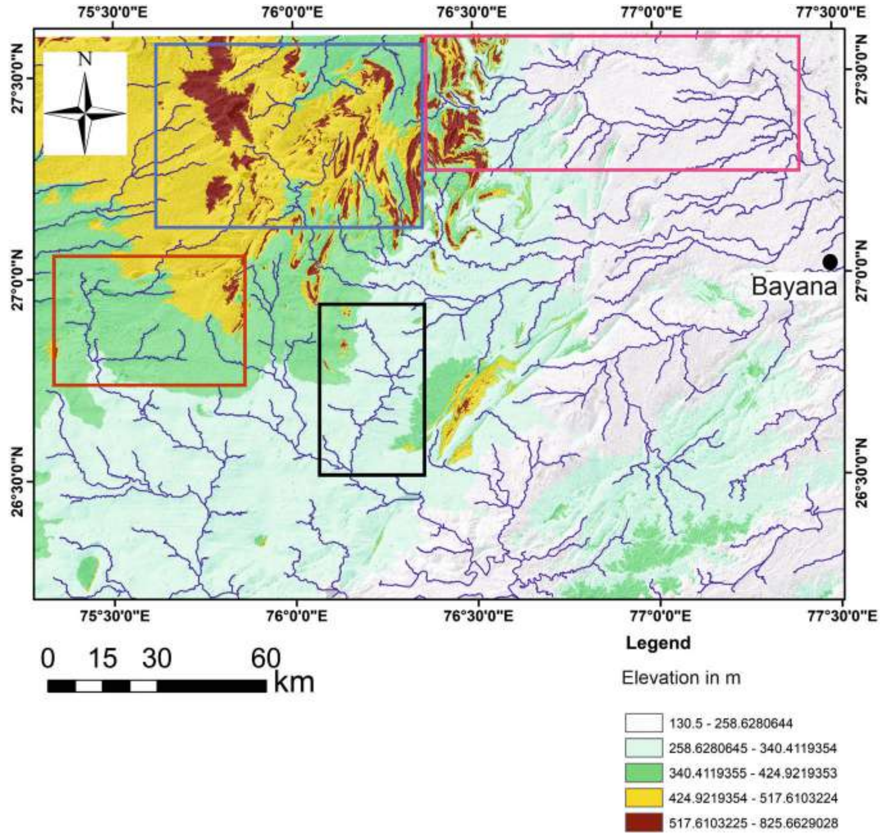

Fig. 3 Elevation map with identified drainage patterns. Drainage patterns- red color box: rectangular; black: trellis; pink: dendritic; blue: radial with angular joining of channels

3.2 Geophysical Aspects

The gravity contour plot (using matrix *g*) for the Bayana region has been plotted (MATLAB 2017 environment) (Fig. 6). The plot shows that the gravity trend varies from −35 to 50 mGal. The study includes five watersheds (W) which show different gravity variations. W4 has the highest gravity values (~ 50 mGal) while the lowest value (~ -35 mGal) has been noticed in W1 and W3. The gravity variation for W2 lies between ~ −20 and ~ 20 mGal. Denser rocks, including basement crystalline rocks or intrusions within the sedimentary sequence, can be linked to positive anomalies in the Bayana basin. Generally, areas with less dense materials or thicker sedimentary sequences are characterized by negative anomalies. These might be associated with areas of the basin that are deeper and have accumulated more sediment (Mishra and Singh, 2006; Nagaraju and Rao, 2014).

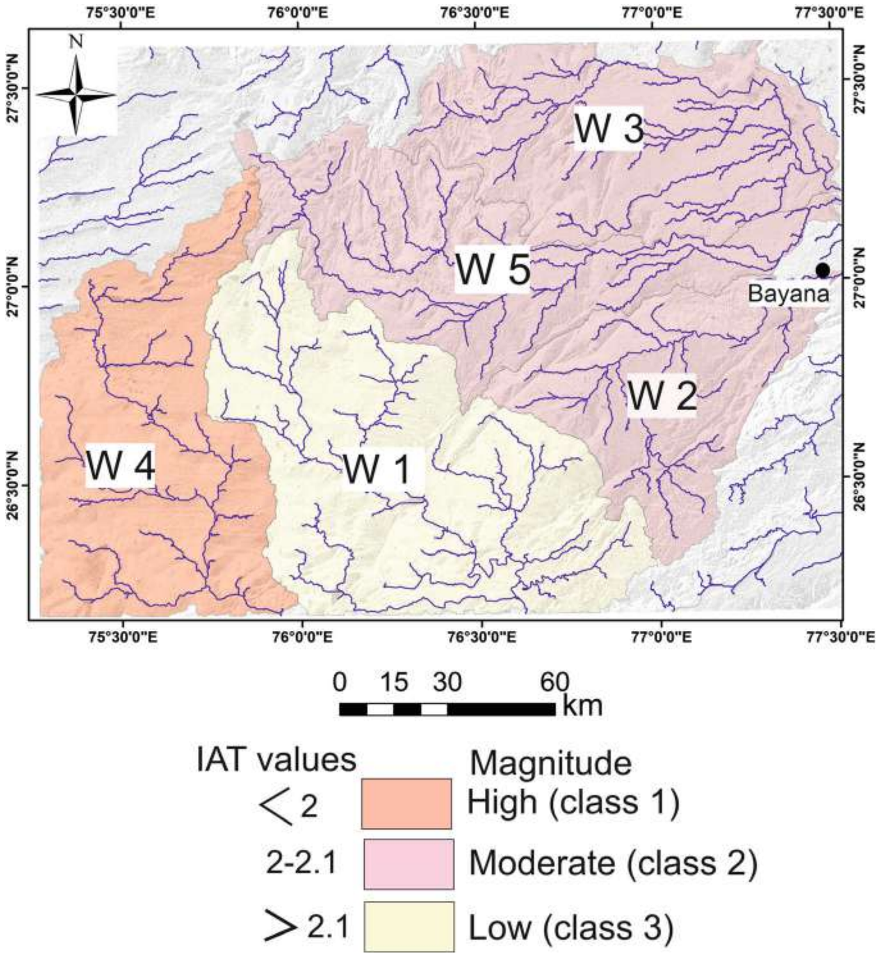

Fig. 4 Map of Index of Active Tectonics (IAT) with three class ranges; class 1 (< 2, tectonically highly active), class 2 (2–2.1, moderate tectonic activity) and class 3 (> 2.1, low tectonic activity). W: watersheds

Now we arrange gravity matrix G (order of 65 × 65) using Eq. (1) and decompose it by the singular value decomposition (SVD) method. The obtained results from the EOF coefficients A_g were in the order of 65 × 65. Here we use the first four A_g and plotted them in Fig. 7. It is well known from linear algebra that the magnitude of A_g coefficients keeps on decreasing from the start and becomes very low till the end. As can be seen from Fig. 7, the A_g (1) magnitude reached up to 200 mGal^2, while the fourth one A_g (4) is only 50 mGal^2.

Bathymetry elevation height data are plotted using MATBALB 2017b version (Fig. 8). The study includes five watersheds that show different elevation heights. The elevation height is lowest around 200 m near Bayana compared to the surrounding

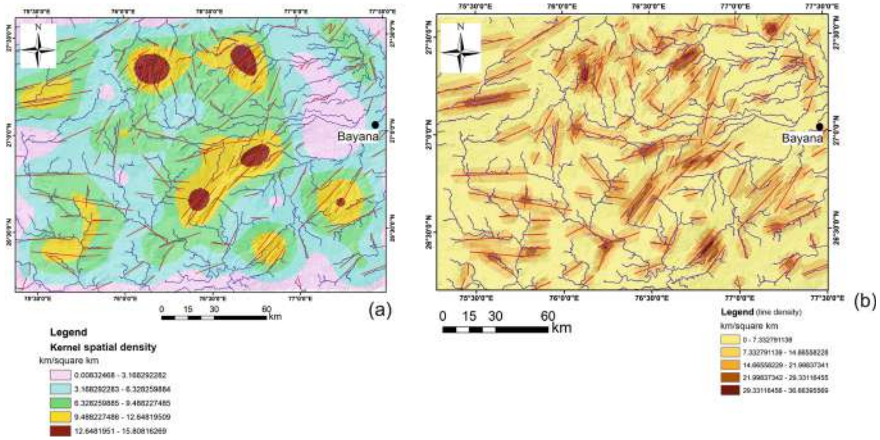

Fig. 5 **a** Kernel spatial lineament density map extracted from DEM hillshade analysis. **b** Line density map of lineaments

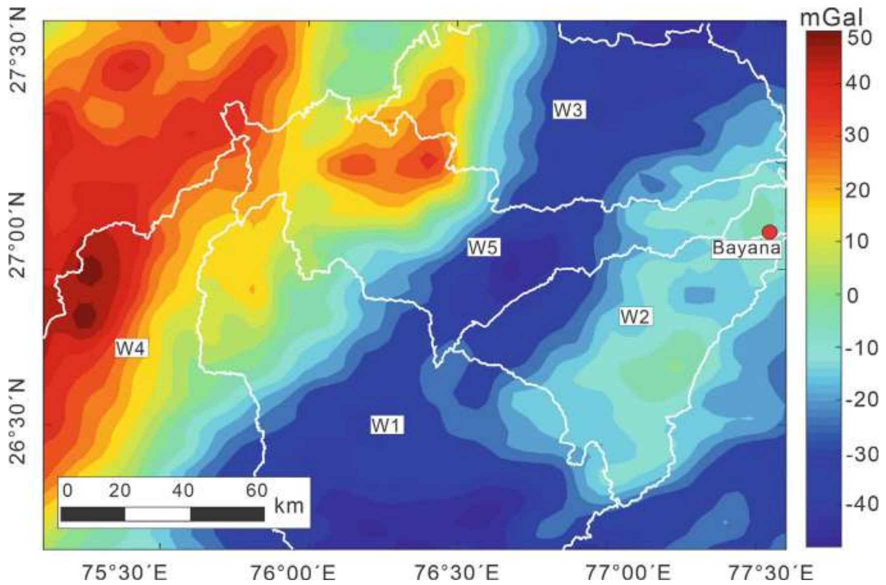

Fig. 6 Regional FAG map of Bayana basin. Color bar: gravity tend (mGal)

region, which reaches up to around 1000 m. This kind of elevated distribution indicates a relatively steep gradient along the basin's eastern flank, while the western side shows a more gradual slope. According to comparisons with historical bathymetric (elevation) data, the basin has changed significantly in the last several decades, most

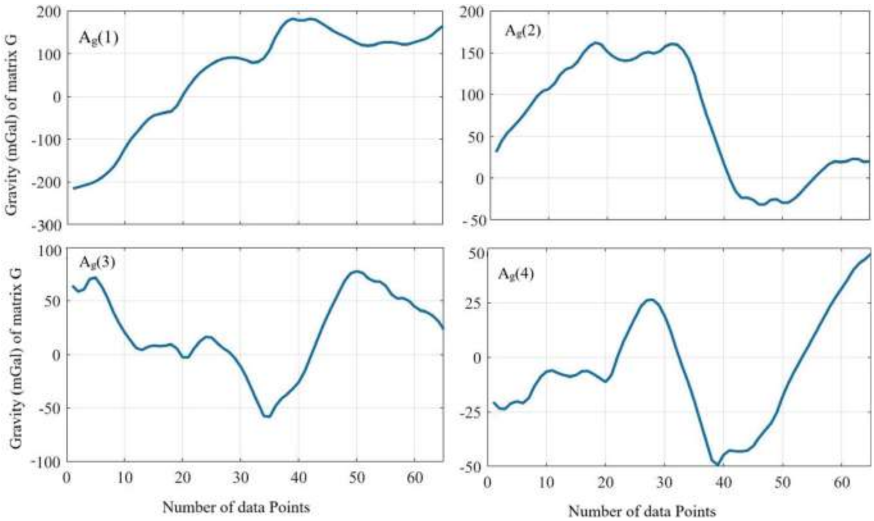

Fig. 7 First four A_g coefficients of matrix G obtained from Eq. (3)

likely because of both natural and man-made processes including dredging and land reclamation projects.

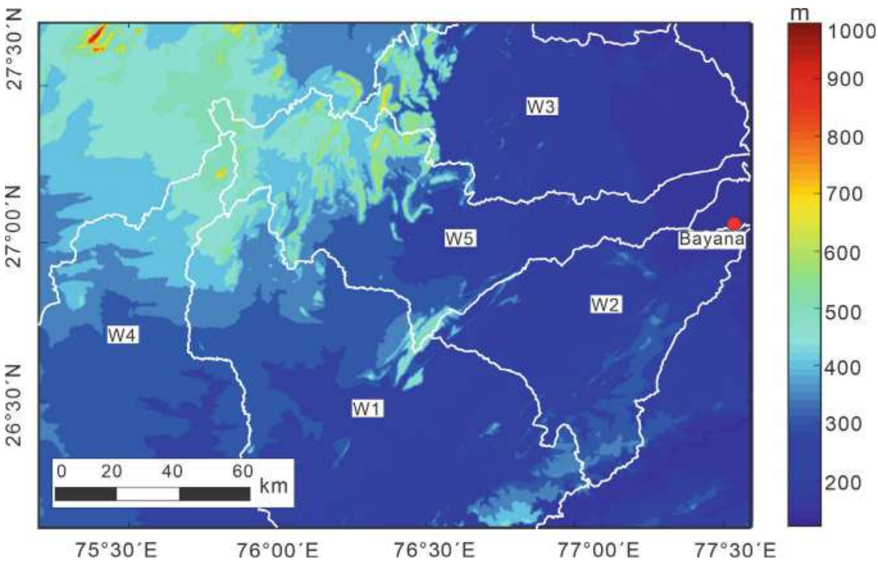

Fig. 8 Regional map of the Bayana basin with plot of bathymetry (elevation) data. Color bar: height in km with respect to the mean sea level (MSL)

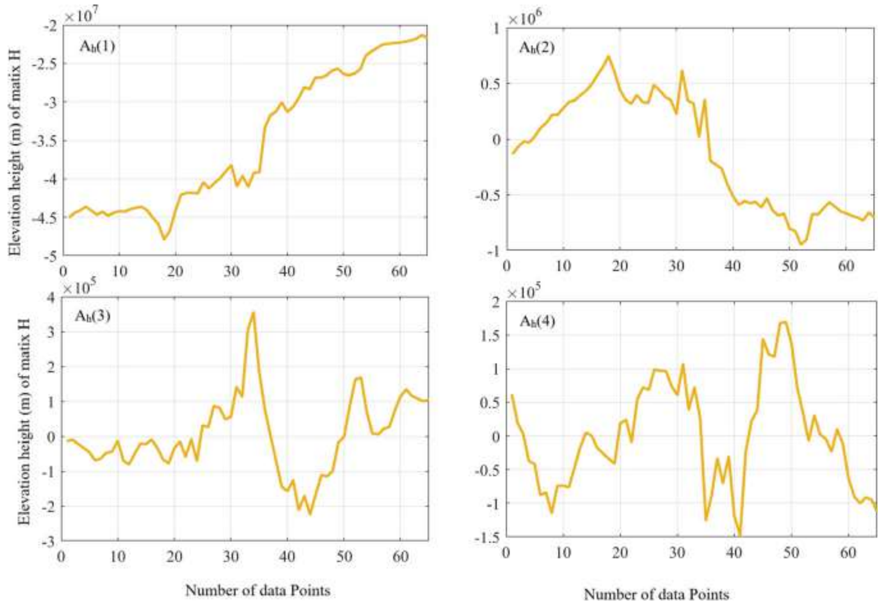

Fig. 9 First four A_h coefficients of matrix H obtained from Eq. (6)

We evaluated the matrix H by using Eq. 4 and estimated Ah from Eq. 6. The first four EOF coefficients A_h are plotted in Fig. 9. Like A_g, we can see from Fig. 9, that A_h (1) highest magnitude reached up to 10^7 m^2 orders, while the fourth one is A_g (4) which is only 10^5 m^2. We selected the densities of crust (ρ_c) and mantle (ρ_m) equal to 2.67 g cm^{-3} and 3.3 g cm^{-3}, respectively (Ganguli and Pal, 2023). In the current study, we selected $d = 42$ km and $k = 0.04$ km^{-1} (Ussami et al., 1993). The value of A_{gb} is calculated from Eq. (9) then put in Eq. (10). The gravity as a function of Bathymetry (g_b) is estimated and then plotted in Fig. 10. The result (g_b) shows almost same kind of trend as it was given by g and is helpful to understand the landscape.

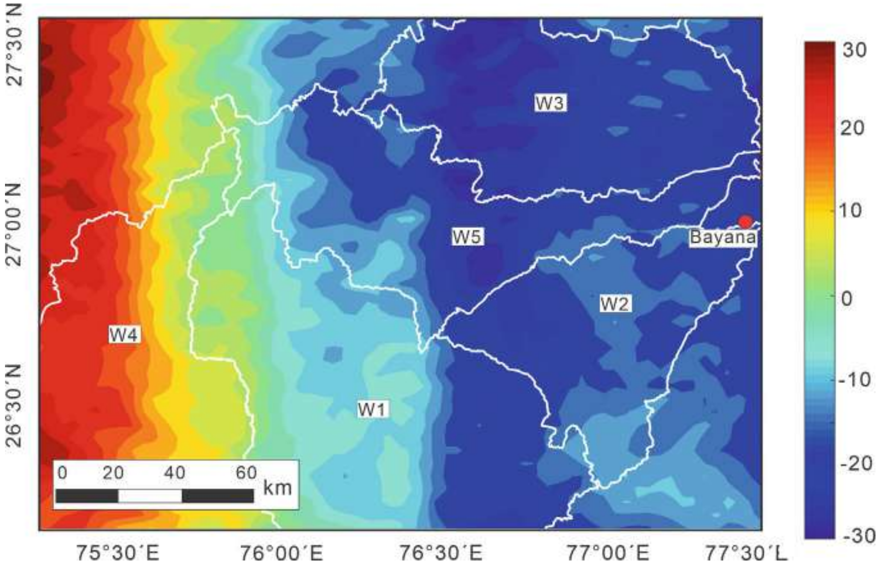

Fig. 10 Regional gravity estimated from Eq. 10 which is a function of Bathymetry map of Bayana basin. Color bar: gravity tend (mGal)

Acknowledgements MB thanks the Department of Geography, Presidency University, Kolkata. SM was supported by internal fund of IIT Bombay. Mukherjee and Kar (2025) summarized this article.

Abbreviations

EOF	Empirical Orthogonal Function
FAG	Free-air Gravity
GEBCO	General Bathymetric Chart of the Oceans
MSL	Mean Sea Level
SVD	Singular Value Decomposition
W	Watershed

References

Ahmad, A.H.M., C. Saikia, and S.M. Wasim. 2012. Petrofacies evolution of Bayana basin sandstones of mesoproterozoic Delhi supergroup, Bharatpur district, Rajasthan. *Northwestern India. Open Journal of Geology* 2: 260.

Ansari, K., J. Walo, S. Sagir, and K. Wezka. 2024. Empirical Orthogonal Function based modelling of ionosphere using Turkish GNSS network. *Journal of Atmospheric and Solar-Terrestrial Physics* 261: 1–8.

Ansari, K., M. Biswas, S. Das, and S. Mukherjee. 2025a. Morphometric, gravity and bathymetric (Topographic) analysis of Bayana basin, Rajasthan, India. In *Geosciences of the Rajasthan basins, India*, ed. S. Mukherjee and N. R. Kar, pp. 43–56. Singapore: Springer. ISBN 978-981-96-3004-2.

Ansari, K., M. Biswas, S. Mukherjee, and Dasgupta. 2025b. Geomorphology, elevation and gravity studies from the western Rajasthan basins (Barmer, Bikaner-Nagaur and Jaisalmer), India. In *Geosciences of the Rajasthan basins, India*, ed. S. Mukherjee and N. R. Kar, pp. 1–18. Singapore: Springer. ISBN 978-981-96-3004-2.

Ansari, K., M. Biswas, S. Das, and S. Mukherjee. 2025c. Morphometric and geophysical studies from a part of Aravalli-Delhi fold belt, Rajasthan, India. In *Geosciences of the Rajasthan basins, India*, ed. S. Mukherjee and N. R. Kar, pp. 57–70. Singapore: Springer. ISBN 978-981-96-3004-2.

Biswas, M., M.P. Gogoi, B. Mondal, T. Sivasankar, S. Mukherjee, and S. Dasgupta. 2022a. Geomorphic assessment of active tectonics in Jaisalmer basin (western Rajasthan, India). *Geocarto International* 37: 12382–12413.

Biswas, M., M.K. Puniya, M.P. Gogoi, S. Dasgupta, S. Mukherjee, and N.R. Kar. 2022b. Morphotectonic analysis of petroliferous Barmer rift basin (Rajasthan, India). *Journal of Earth System Science* 131: 140.

Biswas, M., A. Raha, S. Mukherjee, and V.S. Kotak. 2024. Geomorphic Imprints of Active Tectonics of the Bikaner-Nagaur Petroliferous Rift Basin and its Surroundings (western Rajasthan, India). *Journal of the Geological Society of India* 100: 377–390.

Dasgupta, S., M. Biswas, S. Mukherjee, and R. Chatterjee. 2022. Structural evolution and sediment depositional system along the transform margin- Palar-Pennar basin, Indian east coast. *Journal of Petroleum Science & Engineering* 211: 110155.

Dasgupta, S., S. Mukherjee, N. Vanik, R. Chatterjee, and S.K. Pal. 2023. Paleostress analyses and rift kinematics of the petroliferous Barmer rift basin, western Rajasthan. *India. Marine and Petroleum Geology* 156: 106442.

Dasgupta, S., and S. Mukherjee. 2017. Brittle shear tectonics in a narrow continental rift: Asymmetric non-volcanic Barmer basin (Rajasthan, India). *The Journal of Geology* 125: 561–591.

Dasgupta, S. 2023. Paleostress analyses and tectonic evolution of the Barmer continental rift basin, western Rajasthan, India. Unpublished Ph.D. thesis. IIT (ISM) Dhanbad.

Dasgupta, S., Mukherjee, S., Chatterjee, R. 2024. Tectonics and Geodynamics of a Narrow Continental Rift: Barmer basin, Rajasthan, India. In: Ciner A et al. (Eds) Recent Research on Sedimentology, Stratigraphy, Paleontology, Geochemistry, Volcanology, Tectonics, and Petroleum Geology, Advances in Science, Technology & Innovation. Springer. pp. 223–227.

Ganguli S. S. and Pal S. K. 2023. Gravity-magnetic appraisal of the southern part of the Cauvery Basin Eastern Continental Margin of India (ECMI): Evidence of a volcanic rifted margin. *Frontiers in Earth Science* 11. https://doi.org/10.3389/feart.2023.1190106

Greco, F., F. Riguzzi, and G. Berrino. 2021. Insights into Seismogenetic Areas in Central Italy from Combined Absolute Gravity and GNSS Measurements. *Remote Sensing* 13: 4649.

Gruber, T.H., C. Gerlach, and R. Haagmans. 2012. Intercontinental height datum connection with GOCE and GPS-levelling data. *Journal of Geodetic Science* 2: 270–280.

Ihde, J., L. Sánchez, R. Barzaghi, H. Drewes, C. Foerste, T. Gruber, G. Liebsch, U. Marti, R. Pail, and M. Sideris. 2017. Definition and proposed realization of the International Height Reference System (IHRS). *Surveys in Geophysics* 38: 549–570.

Internet ref-1: http://www.gebco.net/data_and_products. Accessed July 12, 2023.

Internet ref-2: https://bgi.obs-mip.fr/data-products/outils/egm2008-anomaly-maps-visualization/. Accessed July 13, 2023.

Internet ref-3: https://portal.opentopography.org/raster?opentopoID=OTSDEM.032021.4326.3. Accessed July 05, 2024

Jamjareegulgarn, P., K. Ansari, and A. Ameer. 2020. Empirical orthogonal function modeling of total electron content over Nepal and comparison with global ionospheric models. *Acta Astronautica* 177: 497–507.

Kar, N.K., D. Mani, S. Mukherjee, S. Dasgupta, M.K. Puniya, A.K. Kaushik, M. Biswas, and E.V.S.S.K. Babu. 2022. Source rock properties and kerogen decomposition kinetics of Eocene shales from petroliferous Barmer basin, western Rajasthan, India. *Journal of Natural Gas Science and Engineering* 100: 104497.

Kar, N.R., D. Mani, B.S. Seetha, E.V.S.S.K. Babu, S. Mukherjee, S. Dasgupta, and M.K.R. Mudiam. 2025. Biomarker evidence of shifts in Organic provenance and depositional environment of Eocene carbonaceous rocks from petroliferous Barmer basin, Western Rajasthan, India. *Journal of the Geological Society of India* 101: 112–122.

Kumar, S., and R. Kumar. 2012. Geology of the Bayana Basin, Bharatpur District, Rajasthan, India. *Journal of the Geological Society of India* 79: 503–514.

Martinson, D.G., 2018. Empirical orthogonal function (EOF) analysis. Quantitative Methods of Data Analysis for the Physical Sciences and Engineering, pp.495–534.

MATLAB. 2017. https://in.mathworks.com/products/matlab.html

McKenzie, D., W. Yi, and R. Rummel. 2014. Estimates of Te from GOCE data. *Earth and Planetary Science Letters* 399: 116–127.

Miall, A.D. 2006. *The Geology of Fluvial Deposits: Sedimentary Facies, Basin Analysis, and Petroleum Geology*. Springer.

Mishra, D.C., and B. Singh . 2006. Gravity and Magnetic Studies of the Bayana Basin, India: Implications for Tectonic Evolution. *Tectonophysics* 415: 107–116.

Mishra, P., G. Karthikeyan, S. Dash, S. Konar, A.K. Bora, U. Kuila, D.K. Mukhopadhyay, and M.D. Zoback. 2023. In situ stress state in the petroliferous Barmer Basin, northwestern India: A new geomechanical approach. *AAPG Bulletin* 107: 1639–1667.

Mondal, B., M, Biswas, S. Mukherjee and M.A., Shaikh. 2024. Geomorphic signatures and active tectonics in western Saurashtra, Gujarat, India. *Geodesy and Geodynamics* 15: 82–99.

Mukherjee, S., and N.R. Kar. 2025. Introduction to *Geosciences of the Rajasthan basins, India.* Springer. pp. v–viii. Singapore: Springer. ISBN 978-981-96-3004-2.

Nagaraju, M., and P.V. Subba Rao. 2014. Integrated Geophysical Studies of the Bayana Basin and Surrounding Areas: Insights into the Subsurface Structure and Tectonics. *Journal of Earth System Science* 123: 341–352.

Parker, R.L. 1973. The rapid calculation of potential anomalies. *Geophysical Journal International* 31: 447–455.

Puniya, M.K., Kaushik, A.K., Mukherjee, S.**,** Dasgupta, S., Kar, N.K., Biswas, M., Choudhary, R. 2023a. New structural geological input from the Barmer Basin, Rajasthan (India). In: Mukherjee S (Ed) Structural Geology and Tectonics Field Guidebook–Volume 2. Springer Geology. pp. 285–296.

Puniya, M.K., Kaushik, A.K., Mukherjee, S., Kar, N.R., Biswas, M., Choudhury, R. 2023b. Structural Geology and Stability Issue of the Giral Lignite Mine, Rajasthan, India. In: Mukherjee, S. (Ed) Structural Geology and Tectonics Field Guidebook–Volume 2. Springer Geology. pp. 297–310.

Raha, A., M. Biswas, and S. Mukherjee. 2023. Application of TOPSIS model in active tectonic prioritization: Madeira watershed, South America. *Journal of South American Earth Sciences* 129: 104502.

Raha, A., K. Ansari, S. Mukherjee. 2025. Geomorphic and geophysical studies from the Sukri River watersheds, Rajasthan, India. In: Mukherjee S, Kar NR (Eds) Geosciences of the Rajasthan basins, India. pp. 153–168. Singapore: Springer. ISBN 978-981-96-3004-2.

Raza, M., A.H.M. Ahmad, M. Shamim Khan and F. Khan. 2012. Geochemistry and detrital modes of Proterozoic sedimentary rocks, Bayana Basin, north Delhi fold belt: Implications for provenance and source-area weathering. *International Geology Review* 54: 111–129.

Shekar, P.R., and A. Mathew. 2024. Morphometric analysis of watersheds: A comprehensive review of data sources, quality, and geospatial techniques. *Watershed Ecology and the Environment*. https://doi.org/10.1016/j.wsee.2023.12.001.

Siegismund, F. 2013. Assessment of optimally filtered recent geodetic mean dynamic topographies. *Journal of Geophysical Research: Oceans* 118: 108–117.

Smith, W.H.F., and P. Wessel. 1990. Gridding with continuous curvature splines in tension. *Geophysics* 55: 293–305.

Ussami, N., N.C. de Sá, and E.C. Molina. 1993. Gravity map of Brazil: 2. Regional and residual isostatic anomalies and their correlation with major tectonic provinces. *Journal of Geophysical Research: Solid Earth* 98: 2199–2208.

Watts, A.B. 2001. *Isostasy and Flexure of the Lithosphere.* Cambridge University Press.

Zingerle, P., R. Pail, T. Gruber, and X. Oikonomidou. 2020. The combined global gravity field model XGM2019e. *Journal of Geodesy* 94: 66.